Environmental Science & Technology

Article

pubs.acs.org/est

Robust Sensor for Extended Autonomous Measurements of Surface Ocean Dissolved Inorganic Carbon

Andrea J. Fassbender,*[,†,∥] Christopher L. Sabine,[‡] Noah Lawrence-Slavas,[‡] Eric H. De Carlo,[§] Christian Meinig,[‡] and Stacy Maenner Jones[‡]

[†]University of Washington, School of Oceanography, Box 357940, Seattle, Washington 98105, United States

[‡]National Oceanic and Atmospheric Administration, Pacific Marine Environmental Laboratory, Seattle, Washington 98115, United States

[§]University of Hawai'i at Mānoa, School of Ocean and Earth Science and Technology, Honolulu, Hawaii 96822, United States

Supporting Information

ABSTRACT: Ocean carbon monitoring efforts have increased dramatically in the past few decades in response to the need for better marine carbon cycle characterization. Autonomous pH and carbon dioxide (CO_2) sensors capable of yearlong deployments are now commercially available; however, due to their strong covariance, this is the least desirable pair of carbonate system parameters to measure for high-quality, in situ, carbon-cycle studies. To expand the number of tools available for autonomous carbonate system observations, we have developed a robust surface ocean dissolved inorganic carbon (DIC) sensor capable of extended (>year) field deployments with a laboratory determined uncertainty of ±5 μmol kg^{-1}. Results from the first two field tests of this prototype sensor indicate that measurements of DIC are ∼90% more accurate than estimates of DIC calculated from contemporaneous and collocated measurements of pH and CO_2. The improved accuracy from directly measuring DIC gives rise to new opportunities for quantitative, autonomous carbon-cycle studies.

INTRODUCTION

The marine biogeochemical cycles are among the more difficult components of the climate system to characterize and thus project the impacts on, and feedbacks from, climate change. This difficulty largely derives from the challenges in developing robust autonomous marine sensors with the endurance and accuracy needed for long-term observational efforts that can resolve environmental variability at the scale needed for synthesis and modeling work.[1] In the past few decades, increased emphasis on understanding the marine carbon cycle and its feedback mechanisms has led to greater demand for autonomous marine carbon sensors. While advancements have been made in the development of some sensors, there remains a need for the development of additional sensors that provide greater insight into the carbonate system than those currently in existence.

To accurately describe the inorganic carbon chemistry of seawater, two carbonate system parameters must be measured simultaneously. The four carbonate system parameters that have been routinely measured from ships are dissolved inorganic carbon (DIC), total alkalinity (TA), partial pressure of carbon dioxide (pCO_2), and pH. Measurement of any two of these parameters in seawater makes it possible to calculate all other carbonate system parameters using equilibrium constants, temperature, pressure, and salinity.[2,3]

Technological advances over the past decade have led to the development of commercially available autonomous carbon dioxide (CO_2) and pH sensors that are capable of yearlong mooring deployments. These sensors have been particularly helpful in further elucidating the episodic nature of biological productivity and the significance of stochastic environmental variability in altering seawater−carbonate chemistry.[4−9] Continuous and simultaneous observations of two carbonate-system parameters from autonomous platforms will make it possible to learn about the drivers of carbon cycling in remote ocean regions. In addition, times-series of this type will be essential for the development and ground truthing of satellite products that may ultimately resolve the current spatiotemporal gaps in surface ocean carbon monitoring capabilities.[10−12] Unfortunately, the strong covariance between pH and pCO_2 makes this the least desirable pair for constraining seawater−carbonate chemistry.[13−15] In order to advance the current state of

Received: September 25, 2014
Revised: February 15, 2015
Accepted: February 18, 2015

DOI: 10.1021/es5047183
Environ. Sci. Technol. XXXX, XXX, XXX−XXX

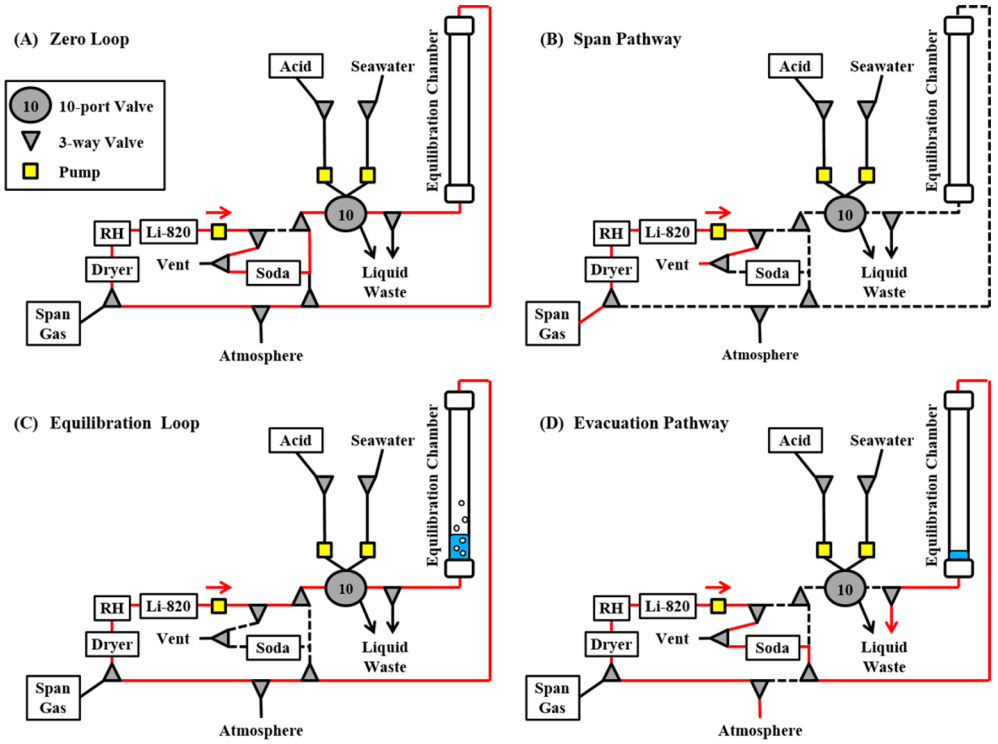

Figure 1. MADIC sensor (A) Zero Loop, (B) Span Pathway, (C) Equilibration Loop, and (D) Evacuation Pathway with gas pathways highlighted in red. A silica gel dryer (Dryer), relative humidity sensor (RH), infrared gas analyzer (LI-820), and two soda lime columns (Soda) can be found along the flow pathways. Liquid and gas flow is controlled by multiple 3-way solenoid latching valves, a 10-port valve, and three diaphragm pumps. Components housed within the instrument are enclosed in solid boxes in the diagram, while waste and external materials are not.

autonomous carbon monitoring capabilities, pH and pCO_2 sensor field accuracies must be improved further, or another carbonate system parameter must be measured in addition to either pH or pCO_2.

We have developed an accurate autonomous DIC sensor that has the endurance required for extended deployments on moorings. DIC is a particularly desirable parameter to characterize because it integrates all of the processes that influence the marine carbonate system, has a larger magnitude response to photosynthesis and respiration than TA, and reflects gas exchange, which TA does not. A number of analytical methods have been utilized for the direct determination of DIC in natural and marine waters.[1,16] Our method includes nearly complete conversion of DIC to CO_2 by acidification, followed by equilibration of the CO_2 in the acidified liquid sample with a closed loop of air, which is quantified using nondispersive infrared (NDIR) spectrophotometry. NDIR spectrophotometry has been utilized by numerous investigators in similar laboratory and ship based techniques[17−26] but has not previously been adapted for an autonomous mooring based DIC sensor. In addition, the NDIR approach is suitable for autonomous operation on a mooring[1] and has the added benefit of being the core technology used in the Moored Autonomous pCO_2 ($MAPCO_2$) system that was originally developed at the Monterey Bay Aquarium Research Institute, improved upon at the Pacific Marine Environmental Laboratory (PMEL) and is now commercially manufactured by Battelle Memorial Institute.[27]

To the best of our knowledge, there have been three published field tests of other autonomous DIC sensors.[16,28,29] These sensors represent substantial progress toward in situ DIC monitoring; however, excluding the 56-day field test described by Sayles and Eck (2009), deployments have thus far been limited to 8 days or less. The sensor we have developed is capable of 2640 in situ analyses, which is equivalent to a 3 hourly sampling frequency over the course of 330 days. Two-way Iridium satellite communication is used to telemeter data back to the laboratory after every two DIC sample measurements allowing for near real-time data delivery and in situ modifications to instrument parameters, such as sampling frequency, in response to changing environmental conditions. Here, we describe this novel Moored Autonomous DIC (MADIC) system and present results from a one month test deployment in Seattle, Washington and a seven month field test near Honolulu, Hawaii.

METHODS

Principle. Dissolved inorganic carbon (DIC) refers to the sum of the concentrations of carbonic acid (H_2CO_3), bicarbonate ion (HCO_3^-), carbonate ion (CO_3^{2-}), and carbon dioxide (CO_2) in aqueous solution. Because it is impractical, and infeasible at this time, to measure each of these molecular species autonomously, our sensor converts DIC into the CO_2 molecular form by acidifying ~1 mL of seawater to a pH of ~3.5. CO_2 in the acidified liquid sample escapes to the gas phase as air, previously stripped of CO_2, is bubbled through the liquid in a recirculating loop. Once equilibrium is reached, CO_2 in the gas phase is measured. The concentration of CO_2 in the gas phase is used with Henry's Law and the Ideal Gas Law to determine the number of moles of carbon in the liquid and gas phases. These numbers are summed and divided by the mass of the injected sample to give the seawater DIC concentration in units of moles per unit mass.

DOI: 10.1021/es5047183
Environ. Sci. Technol. XXXX, XXX, XXX−XXX

Measurement Procedure. The DIC measurement method relies on infrared detection of the mole fraction of CO_2 in air, denoted xCO_2, in units of parts per million (ppm). At the start of each sample measurement, the infrared detector (LI-820) performs a two point calibration at 0 ppm xCO_2 and at a higher xCO_2 value near 1000 ppm; dependent on the calibration gas used. Calibration prior to each measurement is required because the LI-820 response is temperature dependent, and the sensor's temperature stabilization mechanism is disabled to reduce power consumption on the mooring. For the zero calibration, air inside the system is recirculated in the Zero Loop (Figure 1A; including the equilibration chamber) through CO_2-scrubbing soda lime for 30 s before the air pump is turned off and the detector is zeroed. For the high xCO_2 calibration, a compressed calibration gas is flushed through the LI-820 optical chamber in the Span Pathway (Figure 1B) for 30 s before the detector's calibration function is initiated. The LI-820 samples at 2 Hz, and 10 s of CO_2 readings made at atmospheric pressure are averaged for each measurement.

After the LI-820 is calibrated, 8.5% phosphoric acid is pumped through a calibrated-volume (~200 μL) tubing loop on a 10-port valve until the loop has been flushed and filled. The acid is then injected into the equilibration chamber, and air is bubbled through the acid and recirculated in the Zero Loop until all of the CO_2 is removed (~30 s). Seawater from ~1 m depth is pumped through a copper−nickel housed 150 μm intake filter, where it mixes with tributyl tin from an antibiofoulant puck, and into a ~1 mL calibrated-volume tubing loop on the 10-port valve. This loop is flushed with ~30 mL of seawater before the sample is collected and injected into the equilibration chamber. As the seawater and acid mix inside of the equilibration chamber, the pH falls to ~3.5 causing DIC in solution to shift from being mostly bicarbonate to mostly CO_2 (>99%). This rapid transformation of nearly all DIC into the CO_2 form causes CO_2 to escape from the solution into the gas phase. Air inside the instrument that was previously stripped of CO_2 is bubbled through the acidified mixture and recirculated in the Equilibration Loop (Figure 1C) for ~5 min to facilitate the transfer of CO_2 from the liquid into the gas phase. During this process, CO_2 evolved from the ~1 mL acidified seawater sample is diluted throughout the Equilibration Loop volume (~60 mL) resulting in xCO_2 values in the range of ~900−1200 ppm, depending on the sample temperature, salinity, and surface ocean DIC content. At equilibrium, < 2% of the DIC originating from the seawater sample remains in solution, primarily as CO_2. The air circulation pump is turned off and the xCO_2 of the gas phase is measured by the LI-820. The acidified sample is then ejected from the equilibration chamber through the Evacuation Pathway (Figure 1D) and air in the system is stripped of CO_2 before the system is put into an idle rest state until the next sample measurement. The entire measurement sequence takes ~12 min.

Calculation of DIC. The sample DIC concentration is calculated by summing the number of moles of CO_2 in the gas and liquid phases at equilibrium and dividing by the mass of the injected sample. The Ideal Gas Law is used to determine the number of moles of CO_2 in the gas phase (n_{gas}). Because CO_2 is not an ideal gas, the fugacity of CO_2 (fCO_2; atm) is computed, which is a parameter that takes into account intermolecular interactions that occur between nonideal gas molecules.

$$fCO_2 = xCO_2 \times P \times \exp\left[\frac{((B + 2 \times \delta) \times P)}{R \times T}\right] \quad (1)$$

This correction relies on the temperature dependent virial coefficients B and δ, the ideal gas constant (R), and LI-820 measurements of temperature (T), pressure (P), and xCO_2.[3] The Ideal Gas Law may then be applied using fCO_2, R, T, and the laboratory calibrated Equilibration Loop Volume (V_{eq}) to determine the number of moles of CO_2 in the gas phase (n_{gas}).

$$n_{gas} = \frac{fCO_2 \times V_{eq}}{R \times T} \quad (2)$$

Henry's Law is used to calculate the concentration of CO_2 ($[CO_2]$; mol kg^{-1}) in the acidified liquid sample at equilibrium with the gas phase.

$$[CO_2] = K_H \times fCO_2 \quad (3)$$

Henry's constant (K_H; mol kg^{-1} atm^{-1}) is dependent on temperature and salinity,[30] so measurements from an external conductivity-temperature-depth (CTD) recorder are used along with temperature readings from a thermometer housed inside the base of the equilibration chamber to compute K_H for each sample measurement. The number of moles of CO_2 in the liquid phase (n_{liquid}) is equal to the product of $[CO_2]$ and the mass of liquid (kg) in the equilibration chamber.

$$n_{liquid} = (\sigma_{sw} \times v_{sample} + \sigma_{acid} \times v_{acid}) \times [CO_2] \quad (4)$$

The mass of liquid in the equilibrator is derived from empirically determined sample and acid loop volumes (v_{sample}, v_{acid}; m^3) and calculations of seawater and acid density (σ_{sw}, σ_{acid}; kg m^{-3}) based on in situ temperature and salinity measurements. The seawater DIC concentration (mol kg^{-1}) is determined by summing n_{liquid} and n_{gas} and dividing by the mass of the injected sample.

$$DIC = \frac{n_{gas} + n_{liquid}}{\sigma_{sw} \times v_{sample}} \quad (5)$$

Laboratory Calibration and Accuracy. The LI-820 is calibrated in situ at the start of every measurement. To collect repeatable sample and acid volumes for each measurement, a 10-port valve with fixed volume tubing-loops and two distinct flow pathways is utilized (Supporting Information, SI). The sample (v_{sample}) and acid (v_{acid}) loop volumes are determined gravimetrically in the laboratory prior to deployment. The Equilibration Loop volume (V_{eq}) is also determined empirically in the laboratory by connecting the loop to a Ruska high-speed digital pressure controller (Ruska Series 7250xi) and injecting a discrete volume of air from a NIST traceable calibrated Hamilton Gastight syringe (model 1025TLL). The pressure change inside the loop after injection is used with the Ideal Gas Law to determine the loop volume. Although air is not an ideal gas mixture, it behaves nearly identical to an ideal gas near a pressure of 1 atm and temperature of 25 °C, hence a correction is unnecessary.

DIC sensor accuracy is highly dependent on these laboratory volume calibrations. Laboratory measurement uncertainties for v_{sample}, v_{acid}, and V_{eq} are ±0.34%, ±0.69%, and ±0.32% respectively. Sensitivity of the DIC calculation to these uncertainties was determined using a Monte Carlo approach in which the volumes were varied around ~3 standard deviations of their uncertainties in a Gaussian manner for 1000 calculations of DIC. The standard deviation of the

DOI: 10.1021/es5047183
Environ. Sci. Technol. XXXX, XXX, XXX−XXX

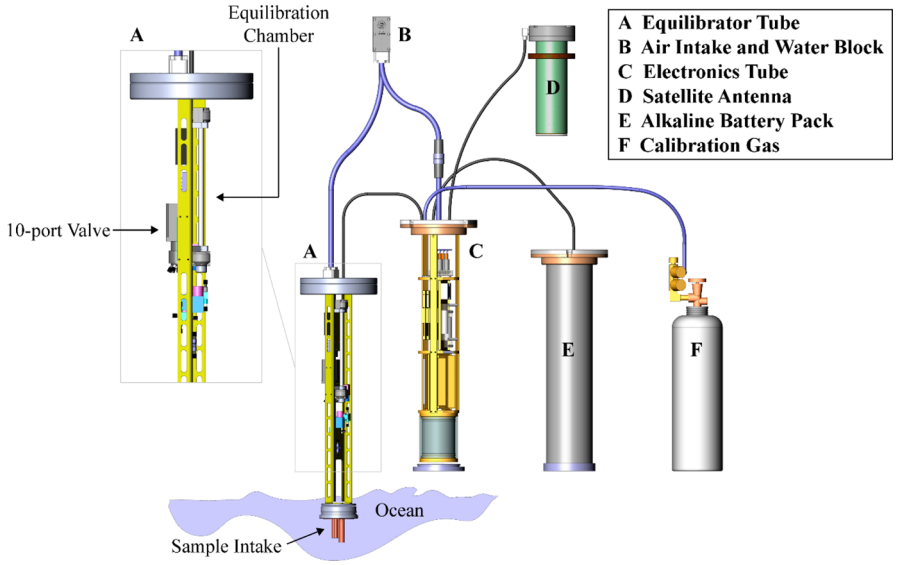

Figure 2. Diagram of the MADIC system. Equilibrator and Electronics Tubes are depicted without the airtight housings used during deployments. A zoom in of the Equilibrator Tube is shown in the upper left to highlight the 10-port valve and equilibration chamber.

resulting 1000 DIC values was then used as an estimate of the theoretical calculation uncertainty. The calculation is most sensitive to the v_{sample} and V_{eq} accuracies, which result in theoretical DIC calculation uncertainties of ±6.5 μmol kg^{-1}. This value is a worst-case scenario because laboratory measurement uncertainty in v_{sample} and V_{eq} is likely larger than the actual variability in these volumes between sample runs.

DIC sensor accuracy was determined in the laboratory by running replicate samples of seawater poisoned with mercuric chloride that was previously analyzed for DIC to ±2 μmol kg^{-1} via coulometry.[31] The reference seawater was measured every 3 h for 3 days (n = 23) yielding an accuracy of 2.5 μmol kg^{-1} with a precision (1σ) of ±5 μmol kg^{-1}, resulting in a sample measurement uncertainty of ±5 μmol kg^{-1}. The primary source of measurement uncertainty during laboratory testing came from inconsistent volumes of liquid being retained in the equilibration chamber after sample evacuation, which influenced V_{eq} and the overall liquid volume between samples.

System Components. The MADIC system was modified from the PMEL MAPCO$_2$ design,[27] and is nearly identical in size, weight, and mounting platform requirements. A custom PMEL ultralow power 332-based controller runs a modified version of PMEL's MAPCO$_2$ firmware. The system interfaces with third party sensors, and provides remote command and control functionality. The average power draw is 0.36 W, and the system will sample autonomously for 330 days, at 8 samples per day, when running off of a MAPCO$_2$ sized battery pack. The sensor is composed of two ∼1 m × 15 cm cylindrical towers (Figure 2). The electronics tube contains a LI-COR LI-820 CO$_2$ gas analyzer and a Sensirion SHT71 relative humidity and temperature sensor. Six ASCO 3-way latching solenoid valves and a Thomas 3003−0312 Pump are used to control gas pathways and flow during different sequences of the measurement. The equilibrator tube contains a Valco 10-port valve and its controller, an acid reservoir, and a 30 cm cylindrical PTFE tube equilibration chamber with an internal diameter (ID) of ∼9.5 mm. A Seabird Electronics (SBE) 38 thermometer is housed (without its case) inside the base of the equilibration chamber to record the temperature of the acidified sample at the time of measurement. Three Takasago 3-way latching solenoid valves are used to control fluid pathways in the equilibrator tube and two KNF Neuberger, Inc. miniature liquid diaphragm pumps are used to pump the acid and seawater sample during measurement cycles. Gas flow pathways linking the electronics and equilibrator tubes are made of ∼1.6 mm ID Zeus PTFE tubing with a small portion of ∼1.6 mm ID Nalgene PVC tubing outfitted with Upchurch Scientific fittings. External temperature and salinity measurements are required to determine the sample density needed for the DIC calculation. A compressed gas cylinder (traceable to World Meteorological Organization standards), antenna, and a battery pack (2900 W-hour Alkaline) are mounted on the buoy. Approximately 0.75 L of 8.5% phosphoric acid is contained within a Pollution Measurement Corporation Tedlar bag with a Tedlar compression tube fitting that is enclosed within a liquid tight Seal Line Padded Storm Sack to protect the Tedlar bag during the deployment. The acid bag is positioned in the base of the instrument housing and is connected directly to a pump with PTFE tubing and Upchurch Scientific fittings.

RESULTS AND DISCUSSION

Field Testing—Seattle Aquarium. The MADIC sensor was first field tested in waters from Washington State's productive Puget Sound estuary using a flow-through system housed in the pump room of the Seattle Aquarium (SI). Water from ∼12 m depth was pumped through a 150 μm mesh filter before entering the flow-through system. The DIC sensor, a SBE 16plus V2 SeaCAT CTD recorder and a SAMI^2-pH unit collected samples every 3 h while a wall mounted General Oceanics CO$_2$ gas analyzer 7000 took xCO$_2$ measurements every 2 min over the course of one month. Twenty discrete bottle samples were collected throughout the deployment and analyzed for DIC via coulometry (±2 μmol kg^{-1}) at PMEL and are considered the highest quality data in this analysis.

In situ DIC measurements are shown in Figure 3A with bottle sample values overlain. The mean difference between MADIC measurements and bottle samples was −6 ± 11 μmol kg^{-1}, indicating that there was not a statistically significant measurement bias. The mean absolute difference between

DOI: 10.1021/es5047183
Environ. Sci. Technol. XXXX, XXX, XXX−XXX

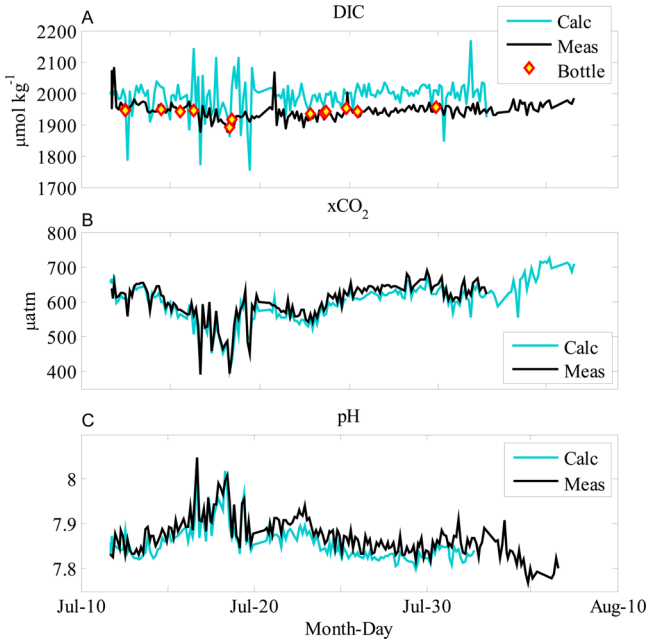

Figure 3. Results from the Seattle Aquarium deployment for (A) DIC (μmol kg^{-1}), (B) xCO$_2$ (μatm) interpolated onto the DIC sample times, and (C) pH. Black lines in each panel are in situ sensor measurements (Meas) and teal lines are values calculated (Calc) from the other two measured parameters using the program CO$_2$sys. Yellow diamonds in subplot **A** are discrete DIC samples.

MADIC measurements and bottle samples was 10 μmol kg^{-1}. The SAMI^2-pH and General Oceanics CO$_2$ gas analyzer 7000 sensors have manufacturer stated accuracies of ±0.003 pH units and ~ ± 4 μatm (±1%) respectively. In situ measurements of pH and xCO$_2$ (Figure 3B,C) were used to calculate DIC concentrations with the program CO$_2$sys[2] using constants from Lueker[32] and Dickson.[33] The calculated DIC values (Figure 3A) have a range of over 300 μmol kg^{-1}; significantly larger than the range observed by the MADIC sensor and bottle samples. The average difference between calculated DIC values and the bottle samples was 52 ± 93 μmol kg^{-1}.[14]

The bias and large variability in calculated DIC may be due to different response times in the pH (~5 min) and xCO$_2$ (~2 min) systems and/or mismatches in the timing of sample readings, particularly during rapid changes in seawater properties.[14] To evaluate the utility of coupling the measured DIC with the other commercially available autonomous sensors, in situ DIC and pH values were used to calculate xCO$_2$, and the DIC-xCO$_2$ pair was used to calculate pH for comparison with the measurements. The calculated xCO$_2$ and pH values (Figure 3B,C) are lower than the measured values (−15 ± 15 μatm and −0.02 ± 0.02, respectively); however, there is good agreement in the temporal variability between measured and calculated values. This indicates that calculations of pH and xCO$_2$ from DIC paired with either of these parameters can reproduce environmental variations, even when considering the flow-through system limitations.

Field Testing—Honolulu, HI. After successful testing in an estuarine environment, the DIC sensor was deployed in a fringing reef environment outside of Kewalo Harbor in Honolulu, HI on October 31, 2013. The MADIC buoy was deployed ~400m from shore in ~13.5m of water and ~25m from an existing MAPCO$_2$ buoy operated by the University of Hawaii and PMEL. A SBE 16plus V2 SeaCAT CTD recorder and a SAMI^2-pH unit were mounted on the buoy bridle. In situ measurements were taken every 3 h for seven months and were timed synchronously with the neighboring MAPCO$_2$ buoy measurements. The buoy and sensors were left unattended for the entire seven month duration of this completely autonomous field test.

The deployment location was selected for three reasons. Stable seawater−carbon chemistry conditions in this region were ideal for testing sensor stability over time.[34] The near shore deployment location made it possible to collect discrete bottle samples via kayak twice per month, with three additional higher-frequency (every 3 h for 24 h) sample collection periods. Finally, colocation of the existing MAPCO$_2$ buoy provided an ideal opportunity to measure three carbonate system parameters continuously over a seven month period for thorough evaluation of the MADIC sensor field performance.

Throughout the deployment, 51 discrete bottle samples were collected next to the MAPCO$_2$ buoy and analyzed for DIC concentration via coulometry (±2−3 μmol kg^{-1}) at the University of Hawaii. Early in the DIC sensor deployment, the xCO$_2$ measurements began to drift over time due to debris in the LI-820 optical path. The xCO$_2$ data were detrended using a linear least-squares regression to account for this drift and a small nonlinear temperature correction was applied (average influence of 1.4 ppm; SI). The resulting instrument and discrete bottle sample DIC concentrations are shown in Figure 4A. The mean difference between the DIC bottle

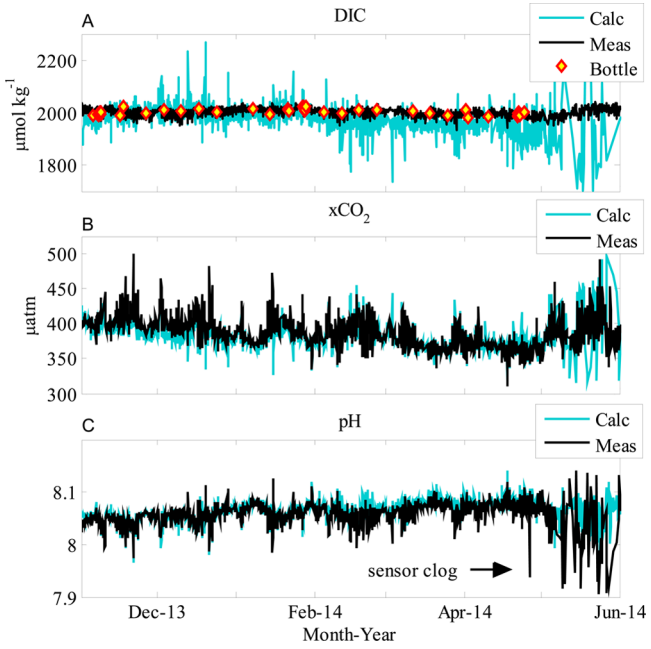

Figure 4. Results from the Honolulu deployment for (A) DIC (μmol kg^{-1}), (B) xCO$_2$ (μatm), and (C) pH. Black lines in each panel are in situ sensor measurements (Meas) and teal lines are values calculated (Calc) from the other two measured parameters using the program CO$_2$sys. Yellow diamonds in subplot **A** are discrete DIC samples.

samples and sensor measurements is 1 ± 11 μmol kg^{-1} (SI), indicating that the MADIC sensor did not show a statistically significant measurement bias throughout the deployment. The mean absolute difference between MADIC measurements and bottle samples was 7 μmol kg^{-1}.

The SAMI^2-pH sensor has a manufacturer stated accuracy of ±0.003 pH units and the MAPCO$_2$ system has a field accuracy

DOI: 10.1021/es5047183
Environ. Sci. Technol. XXXX, XXX, XXX−XXX

of ±2 μatm.[27] In situ measurements of pH and xCO_2 (Figure 4B,C) were used to calculate DIC concentrations with the program CO_2sys.[2] The calculated DIC values (Figure 4A) range over 400 μmol kg^{-1}, well beyond the range of DIC concentrations determined from the MADIC sensor and bottle samples. The average difference between the DIC bottle samples and calculations is 21 ± 37 μmol kg^{-1}. To determine if these errors were due to sensor malfunction, in situ DIC and pH (xCO_2) values were used to calculate xCO_2 (pH) for comparison with the sensor measurements. Agreement between calculated and measured xCO_2 and pH values (−3 ± 9 μatm and 0.006 ± 0.009, excluding May data due to a SAMI^2-pH sensor clog) suggests that neither sensor malfunctioned during the field deployment (Figure 4B,C).

A sustained decrease in the calculated DIC values appears to coincide with a divergence in the measured and calculated pH values around February 2014. This suggests that SAMI^2-pH sensor measurements may have been biased low during the second half of the deployment, likely due to biofouling near the sensor intake, which was covered in growth upon sensor recovery. Disagreement between the measured and calculated DIC values at higher temporal frequencies (~daily) may be due to slight differences in the water being sampled by the pH and xCO_2 sensors, which were mounted on buoys ~25m apart, and/or differing sensor response times. It is possible that better results could be achieved by mounting the sensors on the same buoy; however, it is also likely that this would not result in computations of DIC that exceed the field accuracy of the MADIC system. If laboratory accuracies were attained in the field, then DIC concentrations could be calculated from $MAPCO_2$ and SAMI^2-pH measurements to an accuracy of ~15 μmol kg^{-1} in waters off shore of Honolulu. On the basis of the results herein, this level of accuracy was not achieved during the Honolulu deployment, although it appears that neither sensor malfunctioned (excluding the May SAMI^2-pH sensor clog) and useful environmental data were collected. Increasing the accuracy of pH and xCO_2 sensors and fine-tuning sampling protocols for simultaneous measurement timing and duration may eventually make it possible to achieve high-quality calculated DIC estimates;[35] however, the challenge of further improving autonomous pH and xCO_2 sensor accuracies has limited the utility of this pair for autonomous carbon cycle analyses thus far. Direct measurement of DIC with either xCO_2 or pH would eliminate the need for such challenging sensor advancements, while producing the quality of data needed to constrain the carbonate system with confidence.

Weekly to monthly variations in the DIC concentration near Honolulu tracked seawater density. Superimposed on the lower-frequency variability were intermittent rain events that caused xCO_2 and DIC concentrations to increase, indicating that freshwater runoff from nearby marinas and land was adding carbon to the near shore marine environment (Figure 5). This finding corroborates prior work by Tomlinson et al.[36] near the Ala Wai Canal who identified elevated nutrient and suspended particulate matter concentrations during the first pulse of stormwater runoff. On the basis of xCO_2 data alone, it was challenging to determine whether observed xCO_2 increases during storms were caused by low pH levels or high inorganic carbon content in the freshwater runoff. With the DIC sensor measurements, it became clear that the freshwater runoff contained more inorganic carbon than ambient seawater, and that a transfer of carbon from land to sea was occurring during these events.

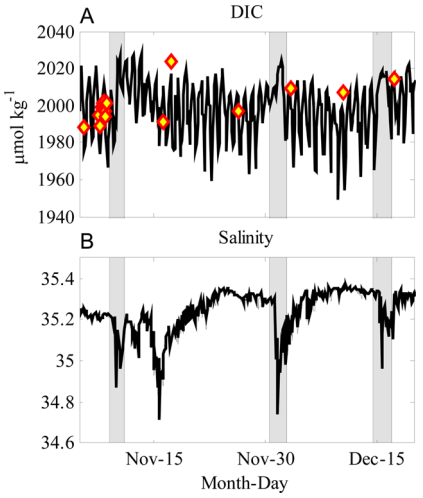

Figure 5. In situ (A) DIC (μmol kg^{-1}) and (B) salinity measurements during November and December 2013 of the Honolulu field deployment. Yellow diamonds in subplot (A) are DIC bottle sample concentrations. Gray regions highlight elevated DIC concentrations associated with rain events.

A distinct diel cycle was found in the DIC time-series, where concentrations were lower during the day and higher at night with an average oscillation magnitude of 17.5 μmol kg^{-1} (Figure 6). Higher diel cycle amplitudes, as previously

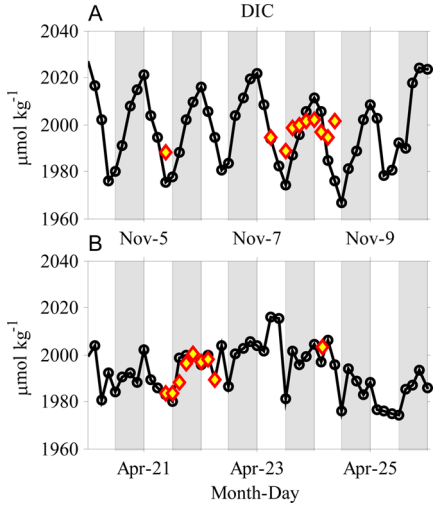

Figure 6. Zoom in on two 6 day periods of the Honolulu DIC (μmol kg^{-1}) time series; (A) at the start of the deployment in 2013 and (B) near the end of the deployment in 2014. Gray bars indicate night time (8pm to 8am local time) and yellow diamonds show DIC bottle sample concentrations.

described by Drupp et al.[34] for other parameters, were observed for DIC during periods of low wind speed (<2 m s^{-1}). This suggests a strong link between the mixed layer stratification that occurs in association with low winds and the magnitude of the diel DIC cycle, as CO_2 gas exchange was found to be negligible in this location under such conditions. The large daily DIC variations are likely caused by calcium carbonate ($CaCO_3$) precipitation and photosynthesis during the day, which decrease the DIC concentration, and $CaCO_3$ dissolution and respiration at night, which increase in the DIC concentration. Interestingly, $CaCO_3$ precipitation results in an increase in

DOI: 10.1021/es5047183
Environ. Sci. Technol. XXXX, XXX, XXX−XXX

xCO_2 (due to the reduction in CO_3^{2-} concentration), which counteracts the effect of photosynthetic xCO_2 drawdown during the day, and $CaCO_3$ dissolution decreases xCO_2, while respiration causes xCO_2 to increase at night. The opposing effects of these processes on xCO_2 result in a muted and more erratic xCO_2 daily cycle, while these processes have an additive effect on the DIC concentration, giving rise to a large daily cycle. As a result, the MADIC sensor may be especially informative in environments where both primary production and calcium carbonate processes are occurring.

Implications. Results from the first two field deployments of the MADIC sensor indicate that DIC sensor measurements are ~90% more accurate (((52−6)/52) = 88%; ((21−1)/21) = 95%) than calculations of DIC from in situ measurements of pH and xCO_2, based on discrete DIC bottle samples. The MADIC sensor did not show any signs of measurement bias or biofouling during the two deployments and provided new insights about seawater−carbon chemistry not obtainable from the pH or xCO_2 sensors alone, or when paired together. The MADIC sensor was robust throughout seven months of unattended field operation, and was still functioning properly at the time of recovery.

Many investigators have engaged in the development of autonomous marine carbon sensors that can be used to better constrain ocean carbon storage and learn about complex carbon cycle feedback mechanisms. As advancement continues, careful consideration of the long-term utility and robustness of these sensors is needed. A growing emphasis on carbon cycle research in coastal seas and high latitude oceans, where freshwater input and sea ice melt can dramatically influence the characteristics of seawater, brings new challenges to the carbon cycle community. pH and TA are carbonate system parameters that have been defined by charge balances that are themselves based on various assumptions about seawater composition that may not hold true in these regions.[3] Direct measurement of DIC may provide clearer information in areas where riverine and freshwater fluxes result in complex carbonate chemistry and observed variations are outside of the range of modern empirically derived definitions and equilibrium constants.

Air−sea CO_2 fluxes have been a powerful way to constrain ocean CO_2 uptake;[37] however, the ultimate goal is to describe changes in the carbon storage of the ocean. As the integrator of all processes influencing seawater inorganic carbon chemistry, DIC is the master variable for ocean carbon storage and cycling studies. Continuous observations of DIC coupled with pH or xCO_2 will make it possible to unravel carbon dynamics in complex and highly variable systems that require continuous monitoring in order to quantify their contribution to the global carbon budget. These systems include areas influenced by rivers or sea ice, coastal upwelling, and areas with significant calcium carbonate production. In such regions, the integrating power of autonomous high-frequency determinations of DIC, which is not biased by carbonate system speciation shifts that can complicate interpretation of pH and xCO_2 signals, will be a powerful measurement tool for studying marine carbon cycling.

■ ASSOCIATED CONTENT

Supporting Information

Details about the 10-port valve flow pathways, Seattle Aquarium flow-through system, and Honolulu, HI drift correction. This material is available free of charge via the Internet at http://pubs.acs.org/.

■ AUTHOR INFORMATION

Corresponding Author

*Phone: (206) 526-6208; fax: (206) 526-6744; e-mail: andrea.fassbender@noaa.gov (A.J.F.).

Present Address

[‖](A.J.F.) National Oceanic and Atmospheric Administration, Pacific Marine Environmental Laboratory, Seattle, Washington 98115, United States.

Notes

The authors declare no competing financial interest.

■ ACKNOWLEDGMENTS

This work was funded by the NOAA Ocean Acidification and Global Carbon Cycle Programs and the NSF IGERT Program on Ocean Change. The authors thank our collaborators at the Settle Aquarium, the Battelle Memorial Institute and at the University of Hawaii including: Ryan Tabata, Patrick Drupp, Jeff Jaeger and Gerianne Terlouw. We also thank our numerous collaborators at PMEL including: Richard Feely, Geoff Lebon, Cathy Cosca, Patrick McLain, Dirk Tagawa, Danna Greeley, Sylvia Musielewicz, Randy Bott, and Joseph Resing. This manuscript has benefited from the insightful comments of three anonymous reviewers and is PMEL contribution number 4234 and SOEST contribution number 9248.

■ REFERENCES

(1) Schuster, U.; Hannides, A.; Mintrop, L.; Körtzinger, A. Sensors and instruments for oceanic dissolved carbon measurements. *Ocean Sci. Discuss.* **2009**, *6*, 491−524 DOI: 10.5194/osd-6-491-2009.

(2) Van Heuven, S. M. A. C.; Pierrot, D.; Rae, J. W. B.; Lewis, E.; Wallace, D. W. R. MATLAB Program Developed for CO_2 System Calculations http://cdiac.ornl.gov/ftp/co2sys/CO2SYS_calc_MATLAB_v1.1/ (accessed Jul 2, 2014).

(3) *Guide to Best Practices for Ocean CO_2 Measurements*; Dickson, A.; Sabine, C.; Christian, J., Eds.; PICES Special Publication 3, 191 pp., 2007.

(4) McGillicuddy, D. J.; Robinson, A.; Siegel, D.; Jannasch, H.; Johnson, R.; Dickey, T.; McNeil, J.; Michaels, A.; Knap, A. Influence of mesoscale eddies on new production in the Sargasso Sea. *Nature* **1998**, *394* ; DOI 10.1038/28367.

(5) McGillicuddy, D. J.; Anderson, L. A.; Bates, N. R.; Bibby, T.; Buesseler, K. O.; Carlson, C. A.; Davis, C. S.; Ewart, C.; Falkowski, P. G.; Goldthwait, S. A.; et al. Eddy/wind interactions stimulate extraordinary mid-ocean plankton blooms. *Science* **2007**, *316*, 1021−1026 DOI: 10.1126/science.1136256.

(6) Karl, D. M.; Laws, E. A.; Morris, P.; Williams, P. J.; Emerson, S. R. Metabolic balance of the open sea. *Nature* **2003**, *426*, 6962 DOI: 10.1038/426032a.

(7) Hales, B.; Karp-Boss, L.; Perlin, A.; Wheeler, P. A. Oxygen production and carbon sequestration in an upwelling coastal margin. *Global Biogeochem. Cycles* **2006**, *20* ; DOI 10.1029/2005GB002517.

(8) Hamme, R.; Webley, P.; Crawford, W. R.; Whitney, F. A.; DeGrandpre, M. D.; Emerson, S. R.; Eriksen, C.; Giesbrecht, K.; Gower, J.; Kavanaugh, M. T.; et al. Volcanic ash fuels anomalous plankton bloom in Subarctic Northeast Pacific. *Geophys. Res. Lett.* **2010**, *37* ; DOI 10.1029/2010GL044629.

(9) Evans, W.; Hales, B.; Strutton, P. G. Seasonal cycle of surface ocean pCO_2 on the Oregon Shelf. *J. Geophys. Res.* **2011**, *116* ; DOI 10.1029/2010JC006625.

(10) Hales, B.; Strutton, P. G.; Saraceno, M.; Letelier, R.; Takahashi, T.; Feely, R. A.; Sabine, C. L.; Chavez, F. P. Satellite-based prediction of pCO_2 in coastal waters of the Eastern North Pacific. *Prog. Oceanogr.* **2012**, *103* ; DOI 10.1016/j.pocean.2012.03.001.

DOI: 10.1021/es5047183
Environ. Sci. Technol. XXXX, XXX, XXX−XXX

(11) Gledhill, D.; Wanninkhof, R.; Eakin, C. M. Observing ocean acidification from space. *Oceanography* **2009**, *22*, 48−59 DOI: 10.5670/oceanog.2009.96.
(12) Friedrich, T.; Oschlies, A. Neural network-based estimates of North Atlantic surface pCO_2 from satellite data: A methodological study. *J. Geophys. Res.* **2009**, *114* ; DOI 10.1029/2007JC004646.
(13) Millero, F. J. The marine inorganic carbon cycle. *Chem. Rev.* **2007**, *107*, 308−341 DOI: 10.1021/cr0503557.
(14) Cullison Gray, S. E.; DeGrandpre, M. D.; Moore, T. S.; Martz, T. R.; Friederich, G.; Johnson, K. S. Applications of in situ pH measurements for inorganic carbon calculations. *Mar. Chem.* **2011**, *125*, 82−90 DOI: 10.1016/j.marchem.2011.02.005.
(15) Dickson, A. G.; Riley, J. The effect of analytical error on the evaluation of the components of the aquatic carbon−dioxide system. *Mar. Chem.* **1978**, *6*, 77−85 DOI: 10.1016/0304-4203(78)90008-7.
(16) Wang, Z. A.; Chu, S. N.; Hoering, K. a. High-frequency spectrophotometric measurements of total dissolved inorganic carbon in seawater. *Environ. Sci. Technol.* **2013**, *47*, 7840−7847 DOI: 10.1021/es400567k.
(17) Broecker, W. S.; Takahashi, T. Calcium carbonate precipitation on the Bahama Banks. *J. Geophys. Res.* **1966**, *71*, 1575−1602 DOI: 10.1029/JZ071i006p01575.
(18) Wong, C. Quantitative analysis of total carbon dioxide in sea water: A new extraction method. *Deep Sea Res. Oceanogr. Abstr.* **1970**, *17*, 9−17 DOI: 10.1016/0011-7471(70)90084-7.
(19) Goulden, P. D. Automated determination of carbon in natural waters. *Water Res.* **1976**, *10*, 487−490 DOI: 10.1016/0043-1354(76)90183-4.
(20) Salonen, K. Rapid and precise determination of total inorganic carbon and some gases in aqueous solutions. *Water Res.* **1981**, *15*, 403−406 DOI: 10.1016/0043-1354(81)90049-X.
(21) Goyet, C.; Snover, A. K. High-accuracy measurements of total dissolved inorganic carbon in the ocean: Comparison of alternate detection methods. *Mar. Chem.* **1993**, *44*, 235−242 DOI: 10.1016/0304-4203(93)90205-3.
(22) Goyet, C. High-accuracy measurements of total dissolved inorganic carbon in the ocean: Comparison of alternate detection methods—A reply. *Mar. Chem.* **1994**, *48*, 89−90.
(23) O'Sullivan, D. W.; Millero, F. J. Continual measurement of the total inorganic carbon in surface seawater. *Mar. Chem.* **1998**, *60*, 75−83 DOI: 10.1016/S0304-4203(97)00079-0.
(24) Kaltin, S.; Haraldsson, C.; Anderson, L. G. A rapid method for determination of total dissolved inorganic carbon in seawater with high accuracy and precision. *Mar. Chem.* **2005**, *96*, 53−60 DOI: 10.1016/j.marchem.2004.10.005.
(25) Bandstra, L.; Hales, B.; Takahashi, T. high-frequency measurements of total CO_2: Method development and first oceanographic observations. *Mar. Chem.* **2006**, *100*, 24−38 DOI: 10.1016/j.marchem.2005.10.009.
(26) Hales, B.; Chipman, D. W.; Takahashi, T. High-frequency measurement of partial pressure and total concentration of carbon dioxide in seawater using microporous hydrophobic membrane contractors. *Limnol. Oceanogr.* **2004**, *2*, 356−364.
(27) Sutton, A. J.; Sabine, C. L.; Maenner-Jones, S.; Lawrence-Slavas, N.; Meinig, C.; Feely, R. A.; Mathis, J. T.; Musielewicz, S.; Bott, R.; McLain, P. D.; et al. A high-frequency atmospheric and seawater pCO_2 data set from 14 open ocean sites using a moored autonomous system. *Earth Syst. Sci. Data Discuss.* **2014**, *7*, 385−418 DOI: 10.5194/essdd-7-385-2014.
(28) Sayles, F. L.; Eck, C. An autonomous instrument for time series analysis of TCO_2 from oceanographic moorings. *Deep Sea Res. Part I Oceanogr. Res. Pap.* **2009**, *56*, 1590−1603 DOI: 10.1016/j.dsr.2009.04.006.
(29) Liu, X.; Byrne, R. H.; Adornato, L.; Yates, K. K.; Kaltenbacher, E.; Ding, X.; Yang, B. In situ spectrophotometric measurement of dissolved inorganic carbon in seawater. *Environ. Sci. Technol.* **2013**, *47*, 11106−11114 DOI: 10.1021/es4014807.
(30) Weiss, R. Carbon dioxide in water and seawater: The solubility of a non-ideal gas. *Mar. Chem.* **1974**, *2*, 203−215 DOI: 10.1016/0304-4203(74)90015-2.
(31) Johnson, K. Coulometric total carbon dioxide analysis for marine studies: Assessment of the quality of total inorganic carbon measurements made during the US Indian Ocean CO_2 survey 1994−1996. *Mar. Chem.* **1998**, *63*, 21−37 DOI: 10.1016/S0304-4203(98)00048-6.
(32) Lueker, T. J.; Dickson, A. G.; Keeling, C. D. Ocean pCO_2 calculated from dissolved inorganic carbon, alkalinity, and equations for K_1 and K_2: Validation based on laboratory measurements of CO_2 in gas and seawater at equilibrium. *Mar. Chem.* **2000**, *70*, 105−119 DOI: 10.1016/S0304-4203(00)00022-0.
(33) Dickson, A. G. Standard potential of the reaction: $AgCl_{(s)} + 1/2H_{2(g)} = Ag_{(s)} + HCl_{(aq)}$, and the standard acidity constant of the ion HSO_4^- in synthetic sea water from 273.15 to 318.15 K. *J. Chem. Thermodyn.* **1990**, 113−127.
(34) Drupp, P. S.; De Carlo, E. H.; Mackenzie, F. T.; Sabine, C. L.; Feely, R. A.; Shamberger, K. E. Comparison of CO_2 dynamics and air−sea gas exchange in differing tropical reef environments. *Aquat. Geochem.* **2013**, *19*, 371−397 DOI: 10.1007/s10498-013-9214-7.
(35) Johnson, K. S.; Berelson, W. M.; Boss, E. S.; Chase, Z.; Claustre, H.; Emerson, S. R.; Gruber, N.; Kortzinger, A.; Perry, M. J.; Riser, S. C. Observing biogeochemical cycles at global scales with profiling floats and gliders: Prospects for a global array. 2009, *22*, 216−225; ; DOI 10.5670/oceanog.2009.81.
(36) Tomlinson, M.; De Carlo, E. H.; McManus, M.; Pawlak, G.; Steward, G.; Sansone, F.; Nicro, O.; Timmerman, R.; Patterson, J.; Jaramillo, S.; et al. Characterizing the effects of two storms on the coastal waters of O'ahu, Hawai'i, using data from the Pacific Islands Ocean Observing System. *Oceanography* **2011**, *23*, 182−199 DOI: 10.5670/oceanog.2011.38.
(37) Takahashi, T.; Sutherland, S. C.; Wanninkhof, R.; Sweeney, C.; Feely, R. A.; Chipman, D. W.; Hales, B.; Friederich, G.; Chavez, F. P.; Sabine, C. L.; et al. Climatological mean and decadal change in surface ocean pCO_2, and net sea−air CO_2 flux over the global oceans. *Deep Sea Res. Part II Top. Stud. Oceanogr.* **2009**, *56*, 554−577 DOI: 10.1016/j.dsr2.2008.12.009.

DOI: 10.1021/es5047183
Environ. Sci. Technol. XXXX, XXX, XXX−XXX